

Electronic supporting information

Electron transfer reaction of TEMPO-based organic radical batteries in different solvent environments: comparing quantum and classical approaches

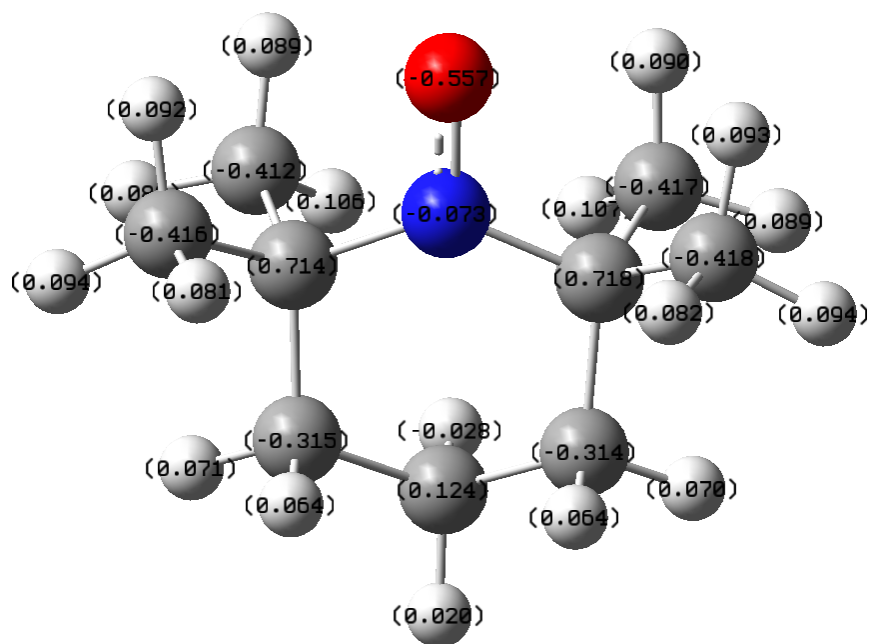
Souvik Mitra,[†] Andreas Heuer,^{‡,†} and Diddo Diddens^{*,‡}

[†]*Institute of Physical Chemistry, Westfälische Wilhelms-Universität Münster, Münster,
48149, Germany*

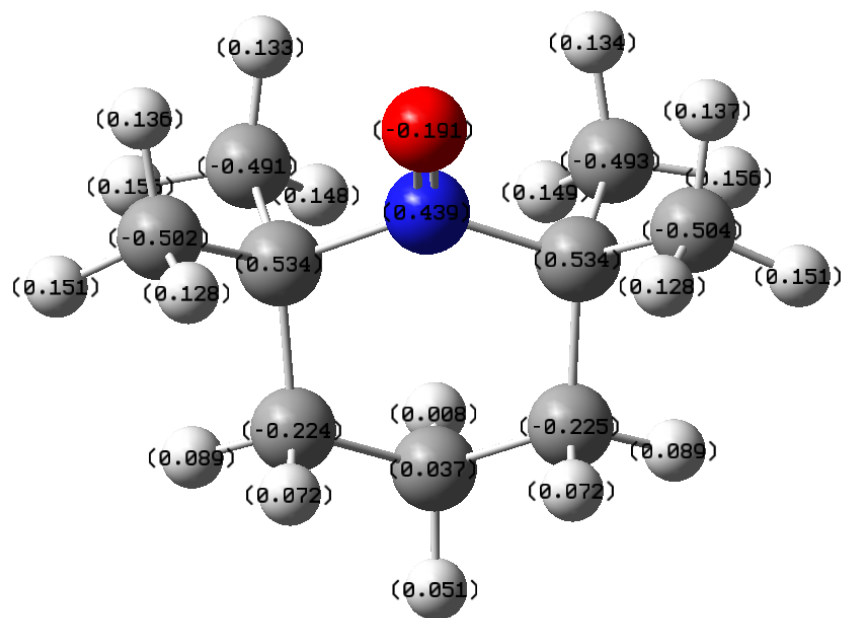
[‡]*Helmholtz-Institute Münster (IEK-12), Forschungszentrum Jülich GmbH, Jülich,
Münster, 48149, Germany, 52425, Germany*

E-mail: d.diddens@fz-juelich.de

Atomic site charges of TEMPO:



(a) TEMPO Radical



(b) TEMPO Cation

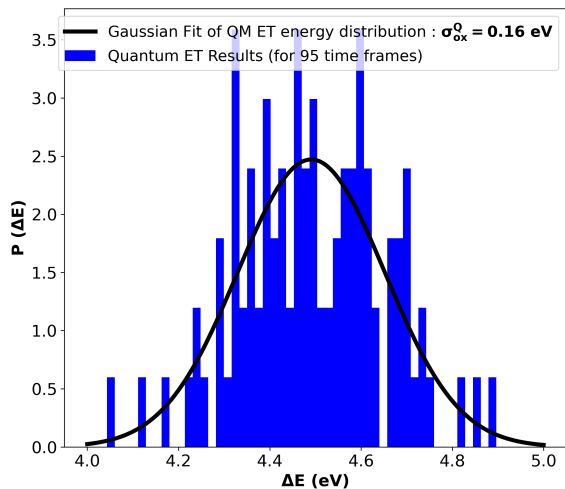
Figure S1: Atomic site charges of (a) TEMPO radical and (b) TEMPO cation from the electrostatic potential (ESP) fit.

Comparison of Vertical Energies (in eV) for Different Functionals in VASP

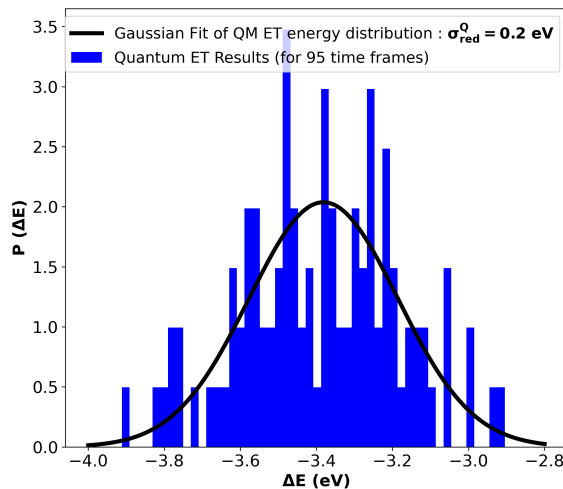
Structure	GGA: PBE	GGA+ Disper- sion correction: PBE+D3	MetaGGA: SCAN
I	3.93	3.94	3.78
II	3.89	3.89	3.83
III	4.04	4.04	4.07

Table S1: Comparison of vertical energies (in eV) for the functionals: (a) PBE, (b) PBE+D3, and (c) SCAN in VASP for three randomly chosen structures from the oxidation of TEMPO radical.

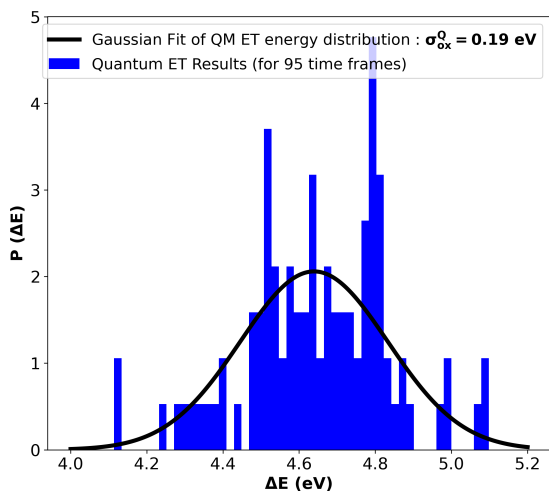
Quantum vertical energy distributions of TEMPO in EC/EMC and EC/EMC/LiPF₆ mixture:



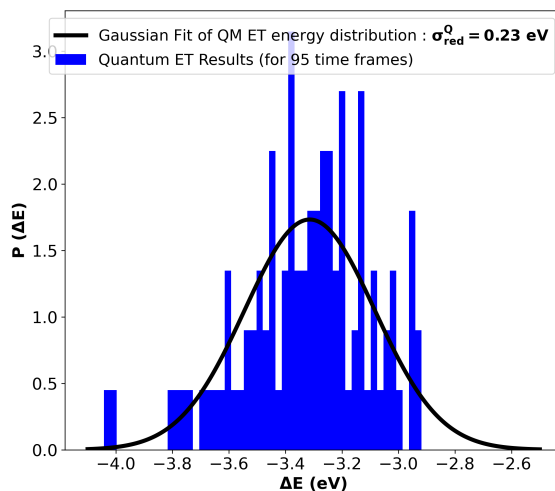
(a) Oxidation of TEMPO· in EC/EMC mixture.



(b) reduction of TEMPO⁺ in EC/EMC mixture.



(c) Oxidation of TEMPO· in EC/EMC/LiPF₆.

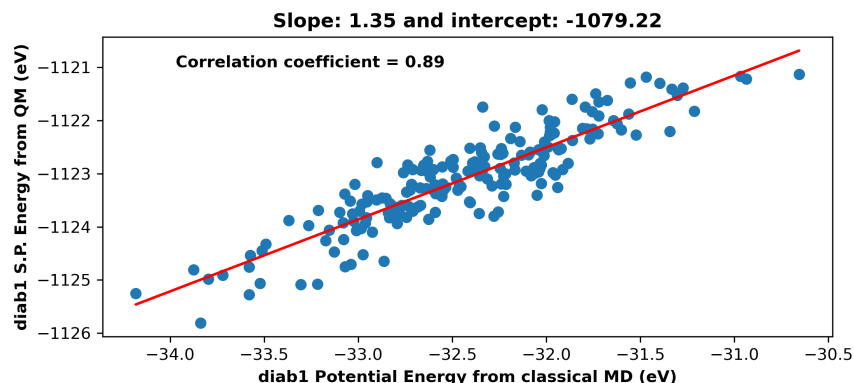


(d) reduction of TEMPO⁺ in EC/EMC/LiPF₆.

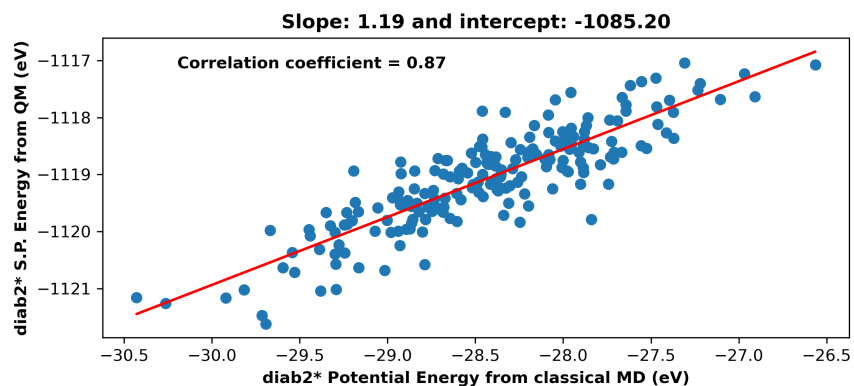
Figure S2: Vertical energy distribution for (a) oxidation of TEMPO· and (b) reduction of TEMPO⁺ in EC/EMC mixture.

Vertical energy distribution for (c) oxidation of TEMPO· and (d) reduction of TEMPO⁺ in EC/EMC/LiPF₆ mixture.

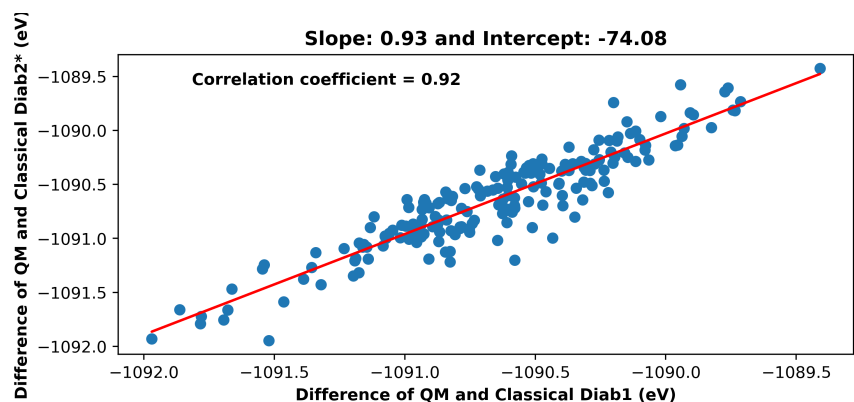
Diabatic state analysis for the oxidation of TEMPO \cdot in water:



(a) Scatter plot between quantum and classical energies in initial charge state (Diab1).



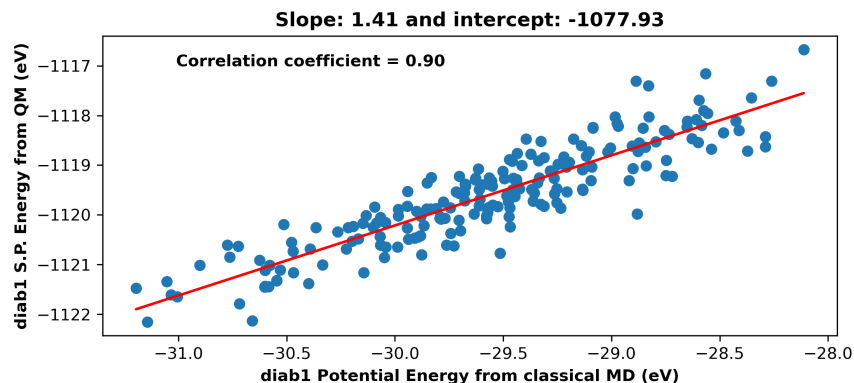
(b) Scatter plot between quantum and classical energies for the structures taken from Diab1 but in final charge state (Diab2*).



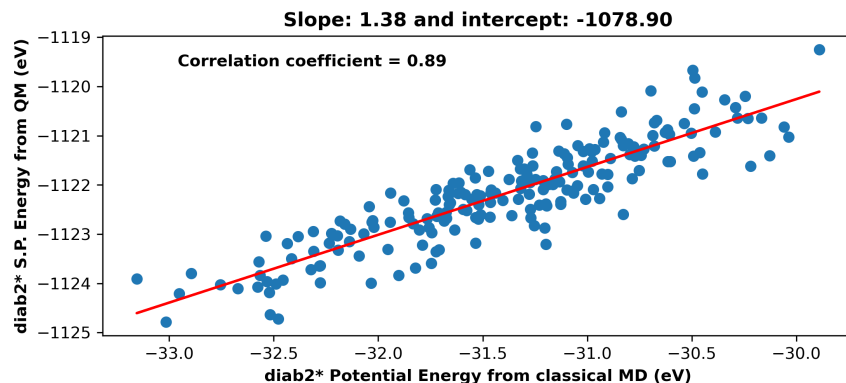
(c) Scatter plot for oxidation of TEMPO \cdot in water.

Figure S3: Scatter plots between classical and quantum results for a) Diab1 state and b) Diab2* state for the oxidation of TEMPO \cdot in water. c) Scatter plots between difference of quantum and classically calculated Diab1 and Diab2*, respectively for oxidation of TEMPO \cdot .

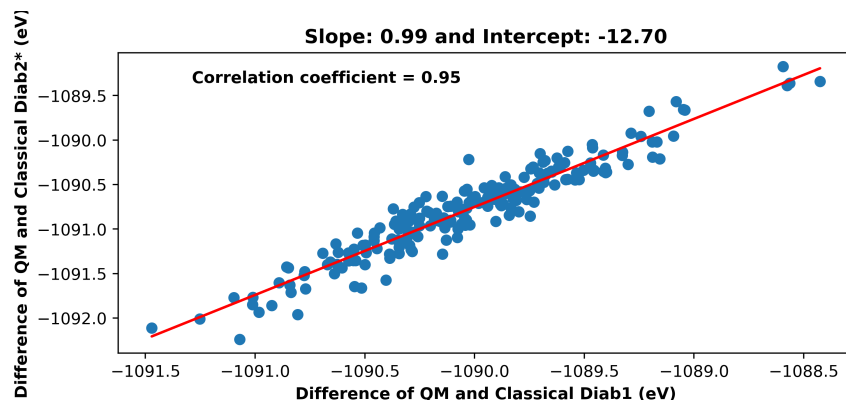
Diabatic state analysis for the reduction of TEMPO⁺ in water:



(a) Scatter plot between quantum and classical energies in initial charge state (Diab1).



(b) Scatter plot between quantum and classical energies for the structures taken from Diab1 but in final charge state (Diab2*).



(c) Scatter plot for reduction of TEMPO⁺ in water.

Figure S4: Scatter plots between classical and quantum results for a) Diab1 state and b) Diab2* state for the reduction of TEMPO⁺ in water. c) Scatter plots between difference of quantum and classically calculated Diab1 and Diab2*, respectively for reduction of TEMPO⁺.

Statistical Insights into the Efficacy of Linear Regression:

In the following section, we examine the correlation coefficient between classical and quantum vertical energies ($\rho_{\Delta E}$) from the relationships between individual diabatic energies (Figure S3 and Figure S4). We denote the quantum energies of the diabatic states 1 and 2 as E_1^Q and E_2^Q , respectively. The corresponding classical energies are denoted as E_1^C and E_2^C .

Based on the high Pearson correlation observed between individual diabatic energies (Figure S3 and Figure S4), we assume a linear relationship between individual diabatic energies, $E_{1/2}^Q$ and $E_{1/2}^C$:

$$E_1^Q = a_1 E_1^C + b_1 + \epsilon_1 \quad (\text{S1a})$$

$$E_2^Q = a_2 E_2^C + b_2 + \epsilon_2 \quad (\text{S1b})$$

Here, $a_{1/2}$, $b_{1/2}$, and $\epsilon_{1/2}$ represent the slope, intercept, and errors, respectively, in the linear regression model for diabatic states 1/2. We assume $\langle \epsilon_1 \rangle = \langle \epsilon_2 \rangle = 0$ by construction of the regression model.

Our goal is to calculate the correlation between quantum and classical vertical energies (ΔE^Q and ΔE^C , respectively). These quantities are defined as follows:

$$\Delta E^Q = E_2^Q - E_1^Q \quad (\text{S2a})$$

$$\Delta E^C = E_2^C - E_1^C \quad (\text{S2b})$$

Expanding the covariance $\langle \Delta E^Q \Delta E^C \rangle$, we obtain:

$$\langle \Delta E^Q \Delta E^C \rangle = \langle E_1^Q E_1^C \rangle - \langle E_1^Q E_2^C \rangle - \langle E_2^Q E_1^C \rangle + \langle E_2^Q E_2^C \rangle \quad (\text{S3})$$

Using Equation S1a and Equation S1b, we can express the covariance of ΔE^Q and ΔE^C as follows:

$$\begin{aligned} \text{Cov}(\Delta E^Q, \Delta E^C) &= a_1 \text{Var}(E_1^C) + a_2 \text{Var}(E_2^C) - (a_1 + a_2) \text{Cov}(E_1^C, E_2^C) \\ &\quad + \langle \epsilon_1 E_1^C \rangle - \langle \epsilon_2 E_1^C \rangle - \langle \epsilon_1 E_2^C \rangle + \langle \epsilon_2 E_2^C \rangle \end{aligned} \quad (\text{S4})$$

Similarly, we can calculate the variance of ΔE^Q as:

$$\begin{aligned} \sigma^{Q^2} &= a_1^2 \text{Var}(E_1^C) + a_2^2 \text{Var}(E_2^C) - 2a_1 a_2 \text{Cov}(E_1^C, E_2^C) \\ &\quad + \text{Var}(\epsilon_1) + \text{Var}(\epsilon_2) - 2\rho_\epsilon \sqrt{\text{Var}(\epsilon_1) \text{Var}(\epsilon_2)} \\ &\quad + 2a_1 \langle \epsilon_1 E_1^C \rangle - 2a_1 \langle \epsilon_2 E_1^C \rangle - 2a_2 \langle \epsilon_1 E_2^C \rangle + 2a_2 \langle \epsilon_2 E_2^C \rangle \end{aligned} \quad (\text{S5})$$

Here, ρ_ϵ is the correlation between ϵ_1 and ϵ_2 .

Similarly, the variance of ΔE^C can be calculated as:

$$\sigma^{C^2} = \text{Var}(E_1^C) + \text{Var}(E_2^C) - 2\text{Cov}(E_1^C, E_2^C) \quad (\text{S6})$$

Finally, from Equations S5, S6, and S4, we can calculate the correlation coefficient between ΔE^Q and ΔE^C ($\rho_{\Delta E}$) using the following expression:

$$\rho_{\Delta E} = \frac{\text{Cov}(\Delta E^Q, \Delta E^C)}{\sigma^C \sigma^Q} \quad (\text{S7})$$

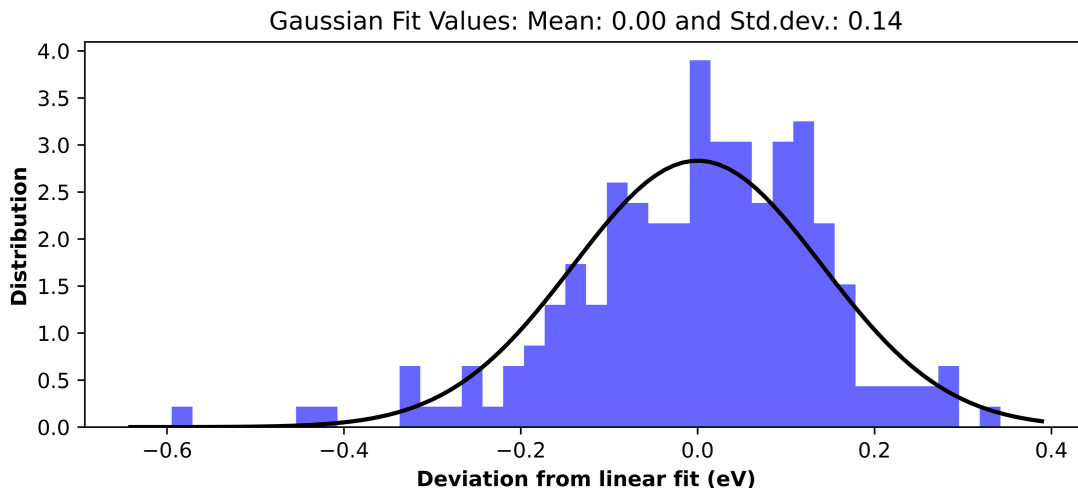
For a qualitative understanding, if one considers $a_1 = a_2 = a'_{diab}$, $\text{Var}(\epsilon_1) = \text{Var}(\epsilon_2) = \Delta$, and assumes that variables $\epsilon_{1/2}$ are independent of variables $E_{1/2}^C$, a relation emerges as follows:

$$\begin{aligned} \rho_{\Delta E} &= \frac{a_{diab} \times \sigma^{C^2}}{[\sigma^{C^2} (a'^2_{diab} \times \sigma^{C^2} + 2\Delta(1 - \rho_\epsilon))]^{1/2}} \\ &= \frac{1}{\left[1 + \frac{2\Delta}{a'^2_{diab} \times \sigma^{C^2}} (1 - \rho_\epsilon)\right]^{1/2}}. \end{aligned} \quad (\text{S8})$$

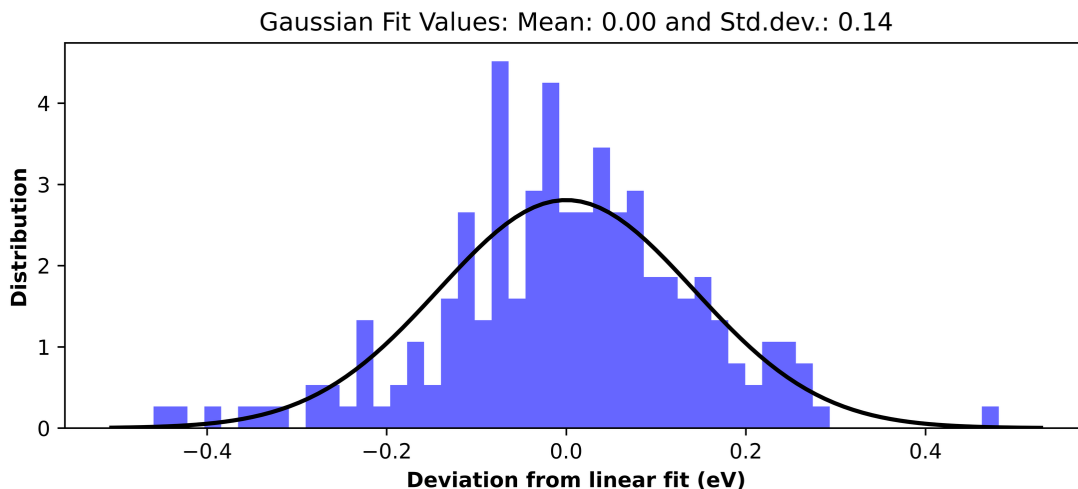
For perfectly correlated error in Equation 11 ($\rho_\epsilon = 1$), the correlation between ΔE^Q and ΔE^C is perfect by construction. If $\rho_\epsilon < 1$ (or even $\rho_\epsilon < 0$), the correlation is weakened, and

this depends on the ratio $\frac{2\Delta}{a'^2_{diab} \times \sigma^{C^2}}$. Therefore, if the variance in the diabatic energy error term (i.e., Δ) is sufficiently small or the product of slope (a'_{diab}) and variance in the ΔE^C (i.e., σ^{C^2}) is sufficiently large, or $\rho_\epsilon \rightarrow 1$, ΔE^Q can be reasonably estimated from ΔE^C .

Error distribution from linear regression for TEMPO in water:



(a) Error distribution for TEMPO \cdot in water.



(b) Error distribution for TEMPO⁺ in water.

Figure S5: Distribution of the variation between the observed quantum vertical energies and their predicted values obtained from the linear fits for (a) oxidation of TEMPO \cdot and (b) reduction of TEMPO⁺.

Scatter plots for vertical energies of TEMPO in EC/EMC and EC/EMC/LiPF₆ mixture:

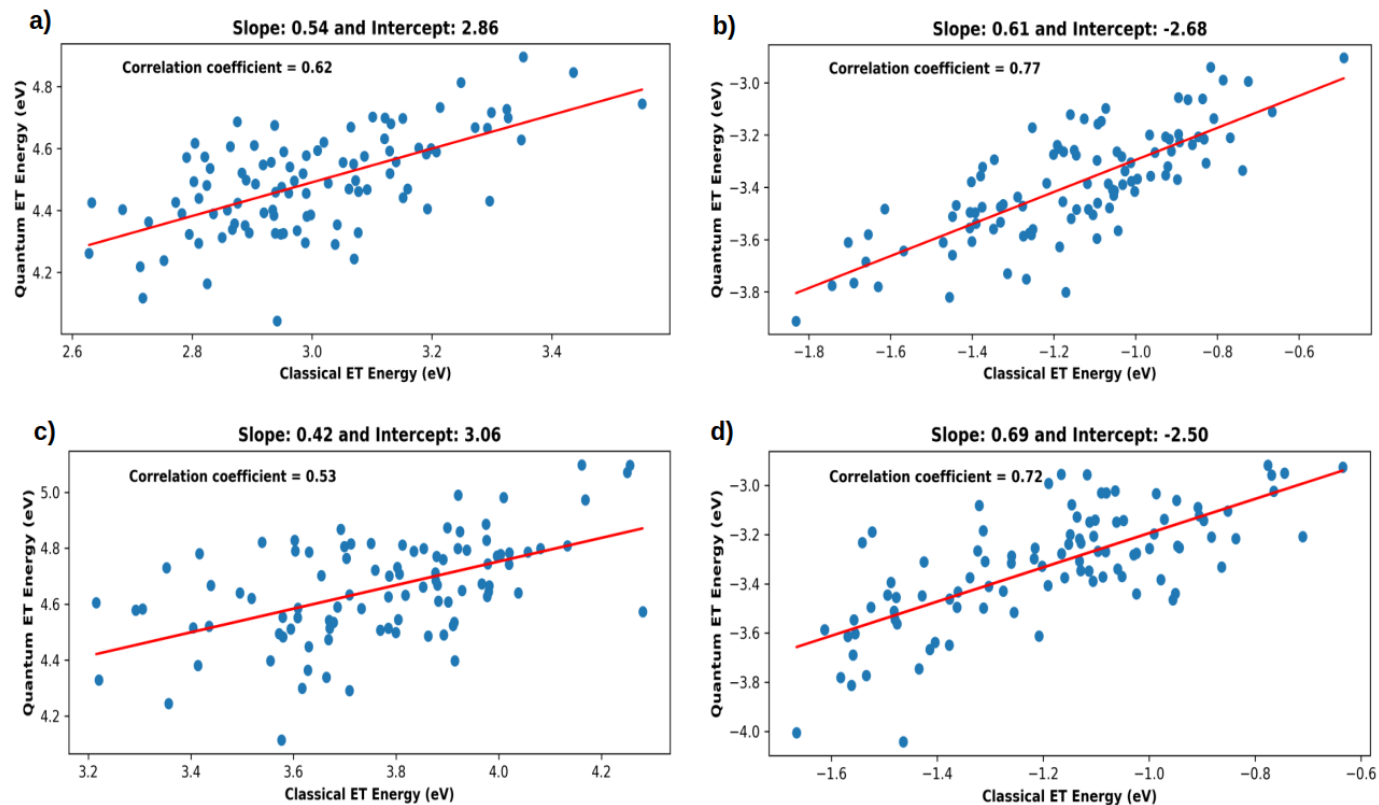
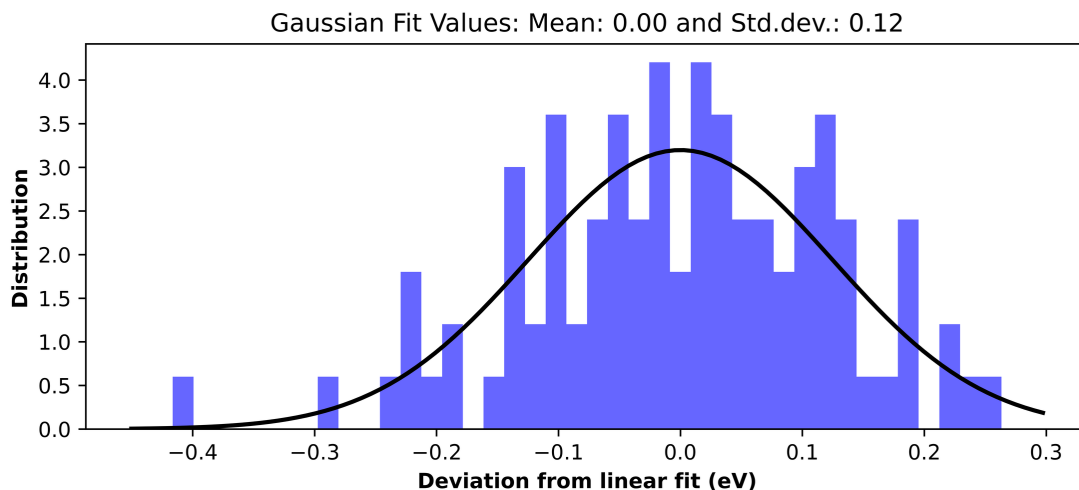
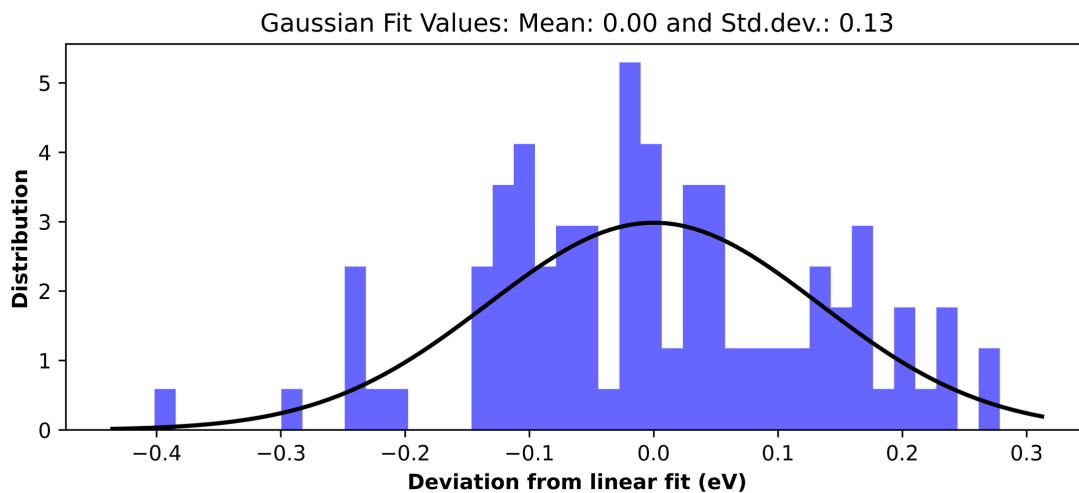


Figure S6: Scatter plots between classical and quantum vertical energies for (a) oxidation of TEMPO[•] and (b) reduction of TEMPO⁺ in EC/EMC mixture. Scatter plots between classical and quantum vertical energies for (c) oxidation of TEMPO[•] and (d) reduction of TEMPO⁺ in EC/EMC/LiPF₆ mixture.

Error distribution from linear regression for TEMPO in EC/EMC mixture:



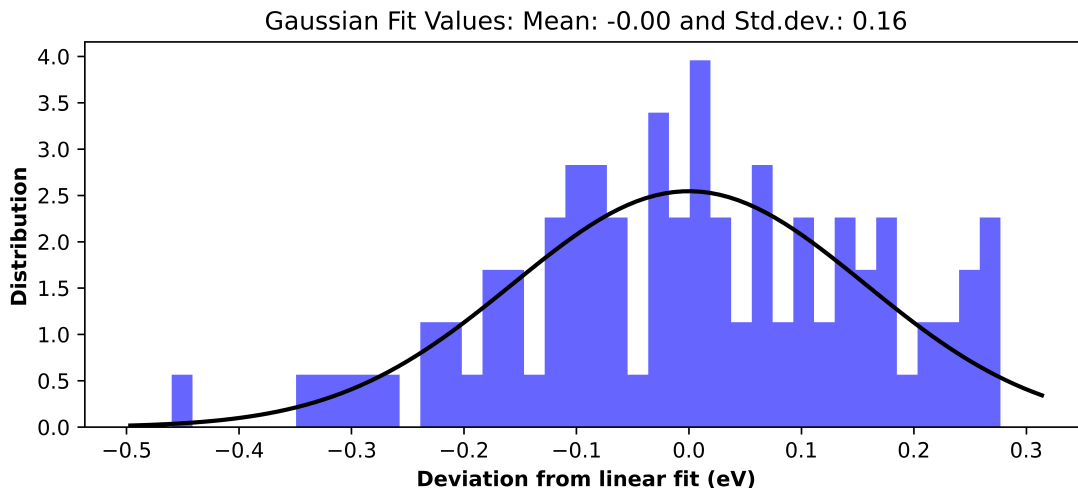
(a) Error distribution for TEMPO \cdot in EC/EMC mixture.



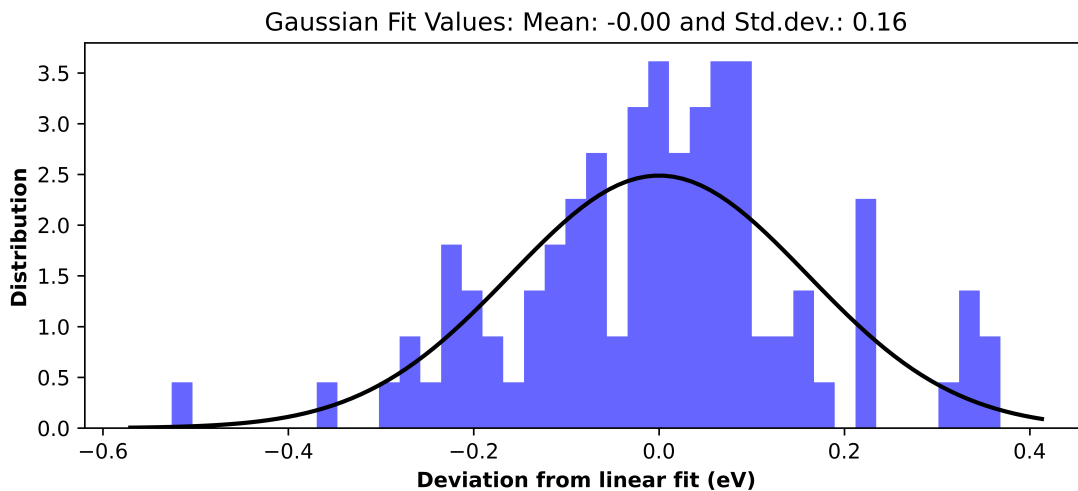
(b) Error distribution for TEMPO⁺ in EC/EMC mixture.

Figure S7: Distribution of the variation between the observed quantum vertical energies and their predicted values obtained from the linear fits for (a) oxidation of TEMPO \cdot and (b) reduction of TEMPO⁺.

Error distribution from linear regression for TEMPO in EC/EMC/LiPF₆ mixture:



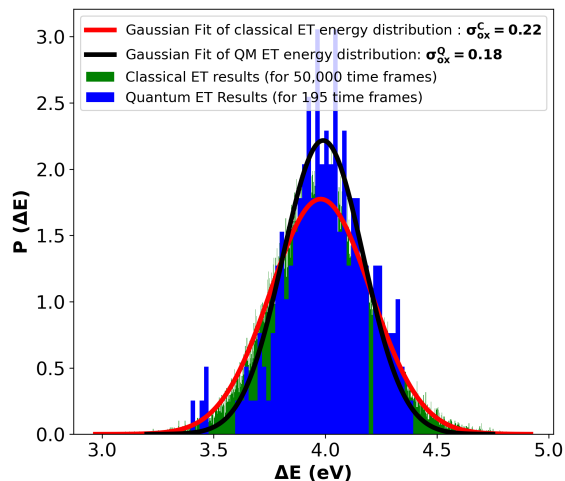
(a) Error distribution for TEMPO \cdot in EC/EMC/LiPF₆ mixture.



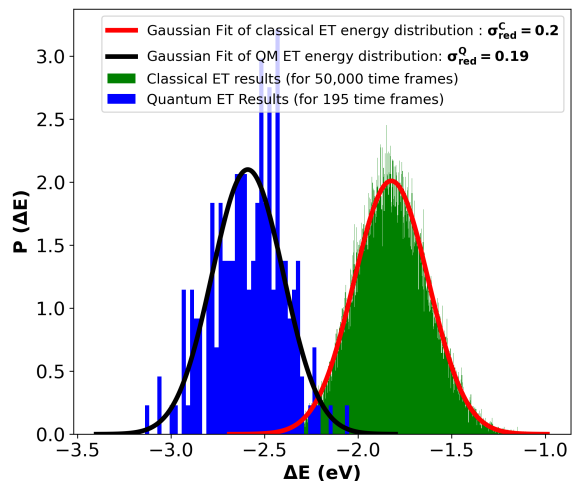
(b) Error distribution for TEMPO $^+$ in EC/EMC/LiPF₆ mixture.

Figure S8: Distribution of the variation between the observed quantum vertical energies and their predicted values obtained from the linear fits for (a) oxidation of TEMPO \cdot and (b) reduction of TEMPO $^+$.

Quantum and Classical vertical energy distributions of TEMPO in water:



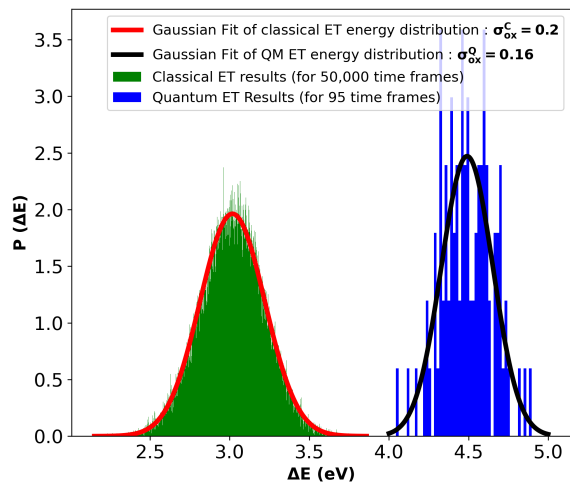
(a) Oxidation of TEMPO·



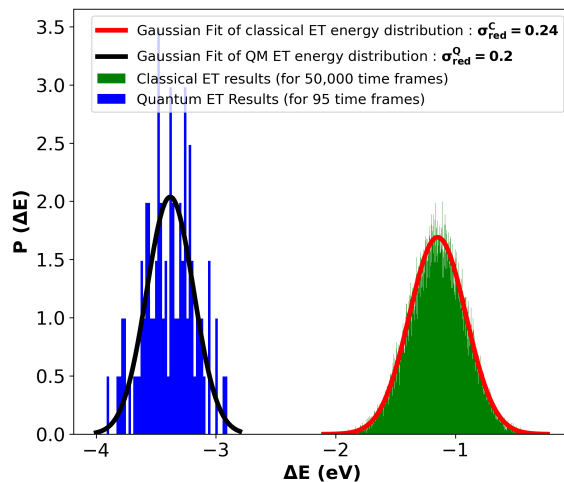
(b) Reduction of TEMPO⁺

Figure S9: Vertical energy distribution a) for the oxidation of TEMPO· in water and b) for the reduction of TEMPO⁺ in water.

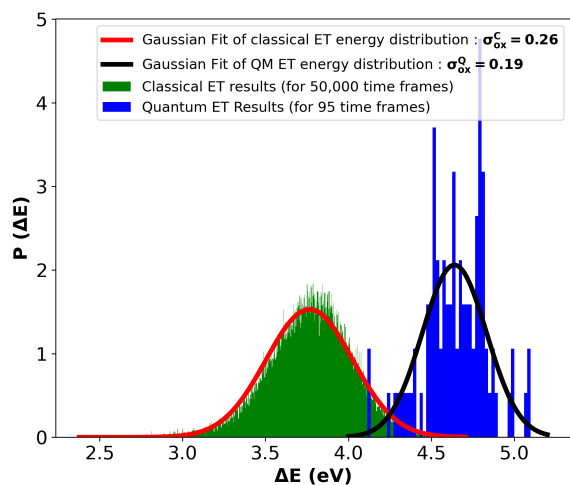
Quantum and Classical vertical energy distributions of TEMPO in EC/EMC and EC/EMC/LiPF₆ mixture:



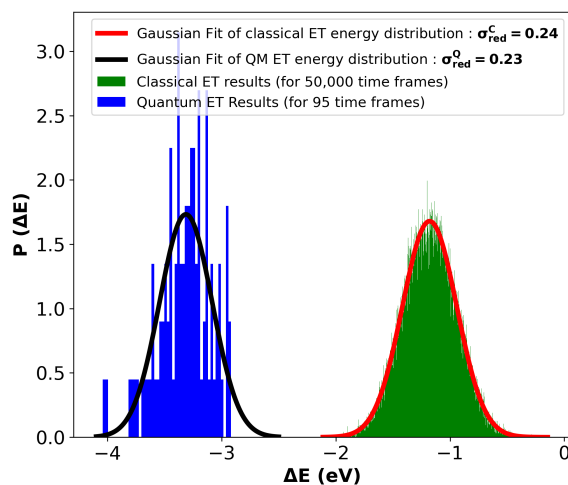
(a) Oxidation of TEMPO \cdot in EC/EMC mixture.



(b) reduction of TEMPO $^+$ in EC/EMC mixture.



(c) Oxidation of TEMPO \cdot in EC/EMC/LiPF₆.



(d) reduction of TEMPO $^+$ in EC/EMC/LiPF₆.

Figure S10: Vertical energy distribution for (a) oxidation of TEMPO \cdot and (b) reduction of TEMPO $^+$ in EC/EMC mixture.

Vertical energy distribution for (c) oxidation of TEMPO \cdot and (d) reduction of TEMPO $^+$ in EC/EMC/LiPF₆ mixture.

RDF plots for EC and EMC w.r.t. Li^+ for TEMPO^+

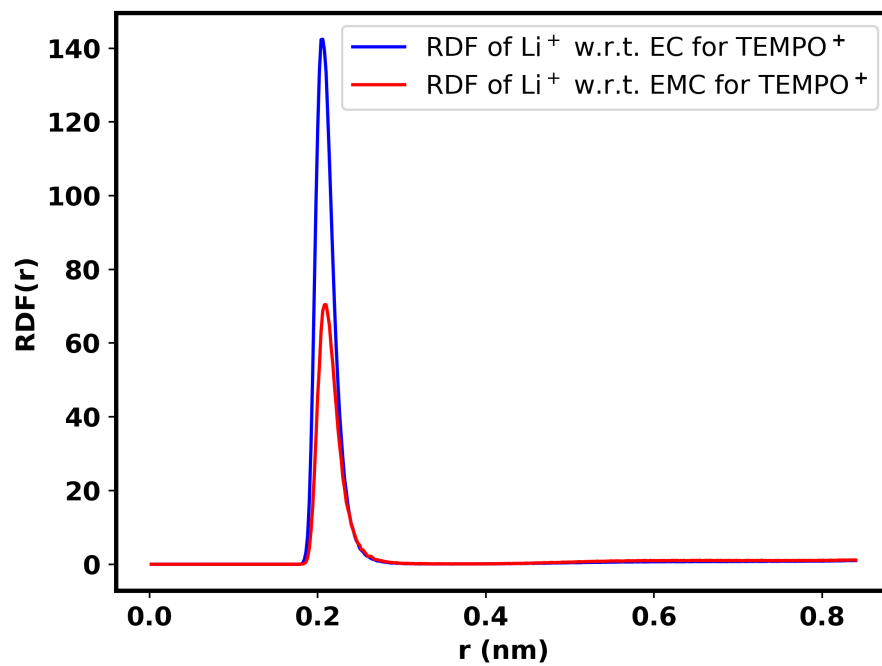


Figure S11: RDF plots for EC (depicted in blue) and EMC (depicted in red) w.r.t. Li^+ for TEMPO^+

RDF plots for EC and EMC w.r.t. Li^+ for TEMPO \cdot .

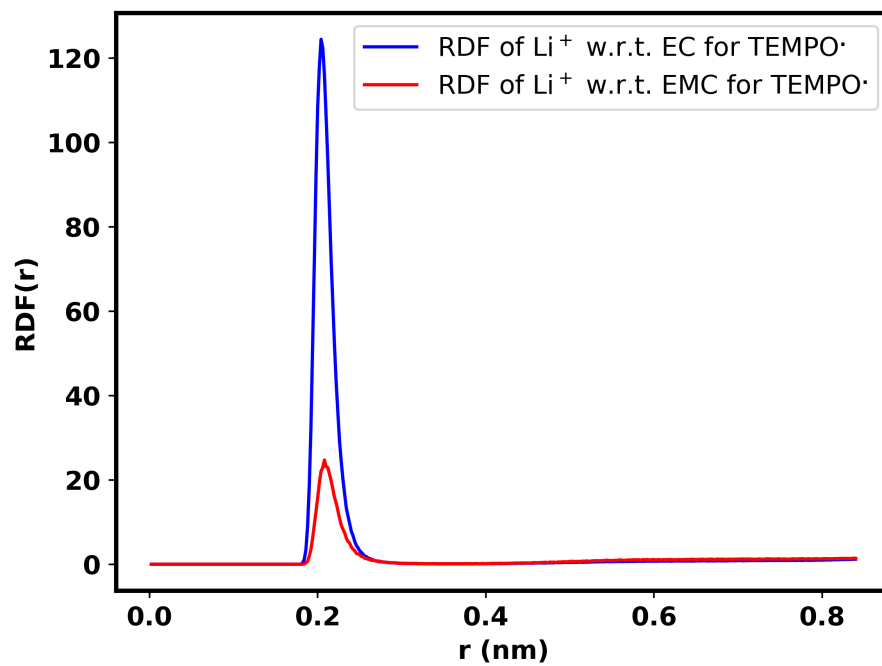


Figure S12: RDF plots for EC (depicted in blue) and EMC (depicted in red) w.r.t. Li^+ for TEMPO \cdot .

RDF plots for Li^+

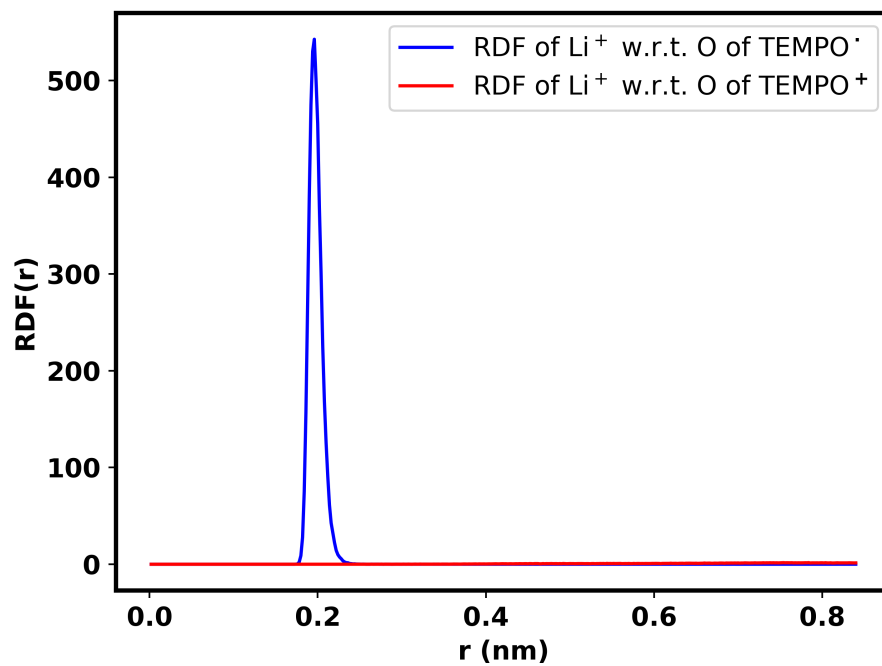


Figure S13: RDF plots for Li^+ w.r.t. TEMPO^\cdot (depicted in blue) and TEMPO^+ (depicted in red).

RDF plots for EC and PF_6^-

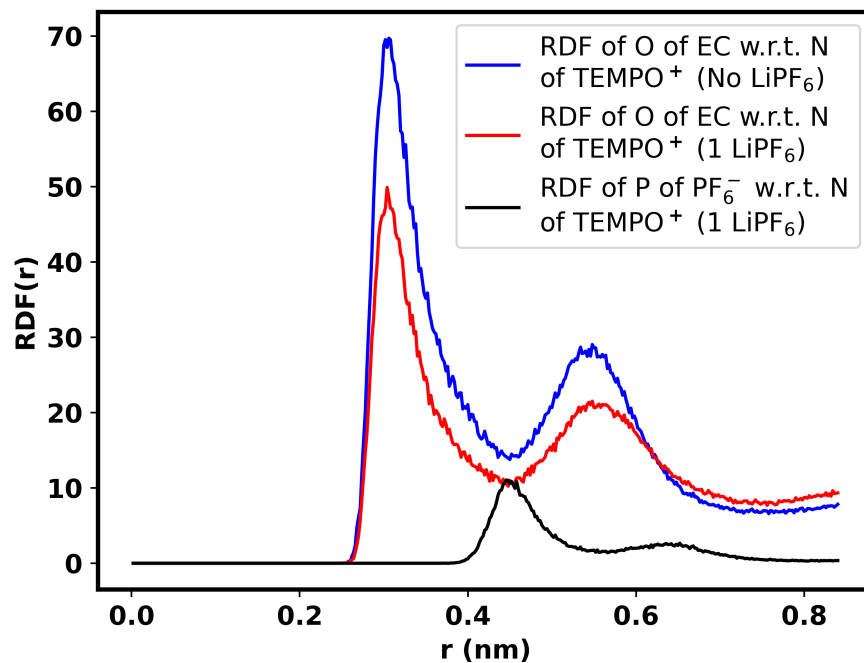


Figure S14: RDF plots for EC w.r.t. TEMPO^+ for both in the presence (depicted in red) and absence (depicted in blue) of LiPF_6 . Along with this rdf plot for PF_6^- w.r.t. TEMPO^+ (depicted in black) is added.